Planetary and Space Science 134 (2016) 82–95

Contents lists available at ScienceDirect

Planetary and Space Science

journal homepage: www.elsevier.com/locate/pss

Dynamical modelling of the Galilean moons for the JUICE mission

D. Dirkx[a,b,*], V. Lainey[c], L.I. Gurvits[a,b], P.N.A.M. Visser[b]

[a] Joint Institute for VLBI ERIC, PO Box 2, 7990 AA Dwingeloo, The Netherlands
[b] Delft University of Technology, Kluyverweg 1, 2629HS Delft, The Netherlands
[c] IMCCE, Observatoire de Paris, PSL Research University, CNRS-UMR8028 du CNRS, UPMC, Lille-1, 77 Av. Denfert-Rochereau, 75014 Paris, France

ARTICLE INFO

Keywords:
Galilean moons
JUICE
Ephemerides
Tidal dissipation

ABSTRACT

Radio tracking and astrometric data obtained by the JUICE mission, using the PRIDE, 3GM and JANUS instruments, will allow the dynamics of the Galilean moons to be measured to unprecedented accuracy. As a result, the dynamical models used for creating ephemerides from these data will most likely require the inclusion of various heretofore neglected physical effects.

To determine which effects will need to be included, we perform a sensitivity analysis of the influence on the dynamics of the system for a wide array of gravitational, tidal and rotational characteristics of the system. We estimate the dynamics of the Galilean moons with a given perturbation turned off, using ideal three-dimensional measurements of the satellites' positions generated with these perturbations turned on. In doing so, we assess the capabilities of the nominal dynamical model to absorb the influence of this perturbations. We analyze the dynamical behaviour over a period of five years, and limit our analysis to effects that may be observable from JUICE radio tracking and optical astrometry data. Our simulations comprise a short-period (5 years) sensitivity analysis of the dynamics of the moons, and *not* a simulation of the tracking data inversion for JUICE.

Our analysis indicates that the nominal dynamical model of the Galilean satellites can very efficiently absorb the influence of the current uncertainties in most of the physical parameters of the Jovian system, to a level where these uncertainties will not be influential for JUICE-derived ephemerides. An important exception is the influence of tidal dissipation: the k_2/Q of Io will be clearly observable by JUICE tracking data, which will be strongly correlated with the weaker effect of Jupiter's k_2/Q. The dissipation inside Europa may also be weakly constrained by JUICE tracking data. Without improvements in the Jovian gravity field from the Juno mission, the estimation of Jupiter zonal gravity field coefficients at degrees 2, 3 and 5 should be included in the ephemerides generation. The influence of the deviation from perfect tidal locking of the moons' rotation is at the limit of observability. Furthermore, we have verified that the present uncertainty in the *a priori* ephemeris of Jupiter will not influence the (Jupiter-centered) dynamics of the Galilean moons at an observable level.

1. Introduction

The dynamical behaviour of (a system of) planetary satellites holds key information on the properties of both the satellites themselves and the central body (e.g. Jacobson, 2004; Emelyanov, 2005; Lainey et al., 2007, 2012; Beauvalet et al., 2012; Folkner et al., 2014; Jacobson, 2014; Lainey et al., 2015). As a result, the dynamical model of these satellites can be used to infer information on their interior structure, composition and rheology, which in turn provides clues to the origin and evolution of both the system under consideration and (exo) planetary systems in general.

So far, the ephemerides of the Galilean system have been based on Earth-based astrometric and mutual event observations, supplemented by both radio tracking and optical data from spacecraft such as Pioneer 10 and 11, Voyager 1 and 2, and Galileo (Lieske, 1980, 1998; Jacobson, 2001; Lainey et al., 2004a, 2009). Optical astrometric observations of the Jovian system, which have an uncertainty of about 20–150 mas, translating to approximately 60–450 km in linear position, are available over a period of over 100 years. The creation of ephemerides from these data has allowed for an estimation of the tidal dissipation in both Jupiter and Io (Lainey et al., 2009).

The dynamical characteristic that dominates the behaviour of the system is the 1:2:4 Laplace mean motion resonance that Io, Europa and Ganymede are locked in. There are several theories on how this resonance came into being (Peale, 1999; Greenberg, 2010), with one key issue being whether the resonance is primordial (e.g., Greenberg, 1987; Peale and Lee, 2002) or whether the satellites evolved into the configuration as a result of tidal dissipation (e.g., Yoder and Peale,

* Corresponding author at: Delft University of Technology, Kluyverweg 1, 2629HS Delft, The Netherlands.
E-mail addresses: D.Dirkx@tudelft.nl (D. Dirkx), Valery.Lainey@imcce.fr (V. Lainey), LGurvits@jive.eu (L.I. Gurvits), P.N.A.M.Visser@tudelft.nl (P.N.A.M. Visser).

http://dx.doi.org/10.1016/j.pss.2016.10.011
Received 13 May 2016; Received in revised form 3 October 2016; Accepted 10 October 2016
Available online 12 October 2016
0032-0633/

1981; Malhotra, 1991). Constraining the properties of both the Jovian moons and Jupiter, especially the tidal characteristics, will be crucial in furthering our understanding of the system's origin and evolution. Furthermore, the present configuration and properties of the Galilean moons can be used to shed insight onto the formation and evolution of the solar system (Deienno et al., 2014; Heller et al., 2015).

The Jupiter Icy Moons Explorer (JUICE) mission is set to arrive in the Jovian system in 2030, focusing on investigation of the Galilean satellites and culminating in a nine-month orbital phase around Ganymede, with a final altitude of 500 km (Grasset et al., 2013; Titov et al., 2014). The data collected by this mission will allow the dynamics of the system to be constrained to revolutionary accuracy. The main instruments that facilitate this are the Planetary Radio Interferometry and Doppler Experiment (PRIDE) (Gurvits et al., 2013) and Gravity and Geophysics of Jupiter and Galilean Moons (3 GM) (Iess, 2013), which will both provide active tracking data obtained from Earth-based radio telescopes. In addition to the Doppler data provided by both systems, 3GM will provide range measurements, which should have an uncertainty of down to 0.2 m. PRIDE will provide uniquely valuable lateral positions of JUICE in the International Celestial Reference Frame (ICRF). These measurements presently have a precision of about 1 nrad (Duev et al., 2012), which translates to a linear position uncertainty of about 750 m (at 5 AU). This could perhaps be improved to the 0.1 nrad level by the use of the Ka-band radio signal (as opposed to the typically used X-band signal) (Lanyi et al., 2007) or in-beam phase-referencing (Fomalont et al., 1999). It is these absolute measurements of range and lateral position that are most valuable for planetary ephemeris generation, as opposed to the Doppler data which are important for reconstructing the trajectory of the spacecraft itself, (e.g., Pitjeva, 2001; Fienga et al., 2009; Jones et al., 2015). The planetary satellite ephemeris generation can benefit from both the absolute and the Doppler data. The precise contribution of each data type will be investigated in future work.

The radio tracking data will be supplemented by the JANUS camera system on JUICE (Jaumann et al., 2013), which will collect astrometric observations of the Jovian moons. This supplements the data available for ephemeris generation, as is done for the generation of Saturnian satellite ephemerides from Cassini data (Lainey et al., 2015). Furthermore, the Gaia mission will provide revolutionary accuracy of the background star catalogue, improving the quality of both past and future ground-based optical astrometry (Arlot et al., 2012). This will result in uncertainties that are no longer limited by the catalogue. This will result in improved uncertainties down to the 10–20 mas level for absolute Earth-based astrometry (Arlot et al., 2012; Robert et al., 2015), a significant improvement over the present state-of-the-art in astrometric data reduction (e.g. Robert et al., 2011). Moreover, the new denser catalogue will allow additional plates to be reduced, for which there are presently insufficient reference stars. Mutual event data, which have a smaller uncertainty than the absolute data, will not be improved as significantly by the Gaia catalogue. However, mutual event data is only sparsely available (once every 6 years), while there is a large volume of historical absolute astrometry. JANUS astrometry will not be improved by the Gaia catalogue, as the uncertainty in its astrometric observables is dominated by the center-of-figure to center-of-mass correction, as discussed by e.g. Pasewaldt et al. (2012). Finally, we note that an improved background catalogue will also be crucial in applying the recently proposed *mutual approximations* in optical astrometry (Morgado et al., 2016) for ephemeris creation. An analysis of the quantitative influence of the Gaia catalogue on all facets of optical astrometry data and the associated improvement in ephemerides and tidal dissipation is yet to be performed, however.

Our goal in this article is to identify the parameters to which the Jovian system may be dynamically sensitive over time scales that are relevant for JUICE observations (nominally 3.5 years). In doing so, we identify those parameters that should or should not be included in the inversion of these data. This will be crucial in optimizing the science observation planning and maximizing the mission's science return. Furthermore, our results provide a guideline for further developments in dynamical modelling of the Galilean moons that may be needed for a robust inversion of the tracking data, in particular those related to tidal and/or rotational properties. We analyze the behaviour of the dynamics over a somewhat longer period of 5 years, to provide a broader context for the results, and improve the robustness of the results on excludability of a given parameter. Also, it allows for a preliminary analysis of the influence of a (short) putative mission extension.

We stress that the analysis in this paper does *not* provide any uncertainties of the physical parameters of the Jovian system that can be estimated using tracking data from the JUICE mission. Such an analysis requires the detailed investigation of the influence of the various tracking data types, mission geometry, observation cadence, etc. Instead, we analyze for which parameters the influence may be visible in the tracking data analysis of the JUICE mission, and for which parameters the influence will be too small and/or indistinguishable from the influence of a change in the initial positions of the moons.

Consequently, we remain independent of any specific tracking observable in this paper, instead analyzing the influence of variations in the system's properties to the overall dynamical behaviour of the moons. In doing so, we build a generic basis upon which future analyses of Jovian-system ephemeris-generation can build, with a focus on the JUICE mission. Nevertheless, our analysis is also relevant for the science return of other planned/proposed missions to the Jovian system, such as Europa Multiple-Flyby Mission (EMFM), (formerly known as Europa Clipper) see (Park et al., 2015) and the Io Volcano Explorer (IVO), discussed by McEwen et al. (2014).

We start in Section 2 by describing our dynamical model. Subsequently, we discuss the approach we use for the sensitivity analysis in Section 3. We present and discuss the results of the sensitivity of the dynamics of the Galilean satellites to the system's physical properties, over a timespan and observational accuracy relevant to JUICE, in Section 4 and summarize our overall conclusions in Section 5.

2. Dynamical models

In this section, we describe the dynamical model we use for the Galilean moons, which is extended from the one used by Lainey et al. (2004b). We limit ourselves to the effects that we expect to be visible at a level that may be relevant for the JUICE mission (Section 3.3).

In Section 2.1, we review the model for mutually gravitationally interacting extended bodies. Subsequently, we present the rotation models we use in Section 2.2 and the model for the tides raised on both Jupiter and the satellites in Section 2.3. Finally, we summarize the present and expected near-future uncertainty in the knowledge of the characteristics of the Jovian system in Section 2.4.

For indices denoting the bodies of the Jovian system, we use i=0 for Jupiter, $i = 1 \ldots 4$ for the Galilean moons (Io, Europa, Ganymede and Callisto, respectively) and $i = 5 \ldots 7$ for Amalthea, Thebe and Himalia, respectively. We propagate the Jovian moons w.r.t. the center of mass of Jupiter, with the orientation fixed w.r.t. the ICRF (J2000). As the initial condition, we use the state of the Galilean moons on January 1, 2030 from the Spice kernel (Acton, 1996) provided by IMCCE (2010), created using the model of Lainey et al. (2009). We use the DE431 solar system ephemeris (Folkner et al., 2014) for positions of the planets and the Sun. We use an extended version (Dirkx, 2015) of the Tudat software toolkit[1] for our numerical simulations.

2.1. Gravitational interaction

Following Lainey et al. (2004b), we denote the potential of a point

[1] http://www.github.com/tudat.

mass of body i, evaluated at point j as $U_{\bar{i}}(\mathbf{r}_j)$ and that of its extended body as $U_{\hat{i}}(\mathbf{r}_j)$. The total potential of the body i is then computed from:

$$U_i(\mathbf{r}_j) = \mu_i(U_{\bar{i}}(\mathbf{r}_j) + U_{\hat{i}}(\mathbf{r}_j)) \tag{1}$$

$$U_{\bar{i}}(\mathbf{r}_j) = \frac{1}{r_{ij}} \tag{2}$$

$$U_{\hat{i}}(\mathbf{r}_j) = \frac{1}{r_{ij}} \sum_{l=2}^{\infty} \sum_{m=0}^{l} \left(\frac{R_{e,i}}{r_{ij}}\right)^l P_{lm}(\sin\phi_{ij})\ldots\ldots(C_{lm}^{(i)}\cos(m\lambda_{ij}) + S_{lm}^{(i)}\sin(m\lambda_{ij})) \tag{3}$$

$$= \sum_{l=0}^{\infty} \sum_{m=0}^{l} U_{\hat{i},lm}(\mathbf{r}_j) \tag{4}$$

where $r_{ij} = |\mathbf{r}_j - \mathbf{r}_j|$ denotes the distance from the center of body i to point j and ϕ_{ij} and λ_{ij} denote the latitude and longitude of point j, as measured from the body-fixed frame of body i. The gravitational parameter of body i is denoted μ_i, the reference radius of the spherical harmonic expansion (typically the equatorial radius) is denoted $R_{e,i}$, P_{lm} is the associated Legendre polynomial of degree l and order m. The (unnormalized) spherical harmonic coefficients $C_{lm}^{(i)}$ and $S_{lm}^{(i)}$ quantify the mass distribution of the body i. In general, these coefficients will be time-dependent due to the tides raised on body i by any number of bodies k, so that:

$$(C, S)_{lm}^{(i)}(t) = (C, S)_{0,lm}^{(i)} + \sum_k \Delta(C, S)_{lm}^{(i,k)}(t) \tag{5}$$

where $\Delta(C, S)^{(i,k)}$ denotes the change in spherical harmonic coefficients of body i, caused by a tide raised by body k (discussed in detail in Section 2.3) and the 0 subscript denotes the nominal gravity field coefficients.

The gravitational acceleration on body i, as exerted by body j, denoted $\ddot{\mathbf{r}}_{ij}$, can be decomposed as the interaction between the point mass and extended bodies i and j as follows:

$$\ddot{\mathbf{r}}_{ij} = \ddot{\mathbf{r}}_{\bar{i}\bar{j}} + \ddot{\mathbf{r}}_{\hat{i}\bar{j}} + \ddot{\mathbf{r}}_{\bar{i}\hat{j}} \tag{6}$$

$$\ddot{\mathbf{r}}_{\bar{i}\bar{j}} = \mu_j \nabla U_{\bar{j}}(\mathbf{r}_i) \tag{7}$$

$$\ddot{\mathbf{r}}_{\bar{i}\hat{j}} = \mu_j \nabla U_{\hat{j}}(\mathbf{r}_i) \tag{8}$$

$$\ddot{\mathbf{r}}_{\hat{i}\bar{j}} = -\mu_j \nabla U_{\hat{i}}(\mathbf{r}_j) \tag{9}$$

We can reasonably neglect the figure-figure interactions $\ddot{\mathbf{r}}_{\hat{i}\hat{j}}$ term (Lainey et al., 2004b; Mathis and Le Poncin-Lafitte, 2009), even considering JUICE's level of measurement accuracy. This assumption is further reinforced by the results shown in Section 4.2 regarding the (lack of) observability of even the $\ddot{\mathbf{r}}_{\hat{i}\bar{j}}$ acceleration on the moons.

2.2. Rotation models

The rotation of each of the Galilean moons is tidally locked, so that their rotation axes have small obliquity and $\dot{\theta}_j \approx n_j$ for the longitudinal rotation angle θ_j of body j, with n_j the mean orbital motion of body j.

Dynamical models of the Jovian system used to fit spacecraft tracking and astrometry data (Section 1) have so far assumed that $\lambda_{j0} = 0$ for each of the Jovian moons during their orbit. However, due to the eccentricity of the orbits of the satellites, this angle will undergo small variations of approximately $f_j - M_j$, with f_j the orbit true anomaly, (Fig. 1). Furthermore, torques acting upon body j will cause librations, denoted $\gamma_{,j}$, so that (e.g. (Van Hoolst et al., 2013)):

$$\psi_j = f - M - \gamma_{,j} \approx 2e\sin(M) - \gamma_{,j}(t) \tag{10}$$

Since the obliquity of the satellites is small, $\psi_j \approx \lambda_{j0}$, with the 0 index denoting Jupiter.

We will limit ourselves to modelling a once-*per*-orbit libration, assuming it to be in phase with the orbital motion. To allow for the adjustment of the ephemerides of the Galilean satellites, while keeping the rotation model consistent with the orbits (i.e. ensuring $<\psi_j = 0>$ over long time intervals), we do not use a fixed *a priori* rotation model, such as that provided by Rambaux et al. (2011). Such an approach was found by Dirkx et al. (2014) to lead to issues with the adjustment of the orbits from highly accurate tracking data (in the case of the Martian moons). Instead, we define the instantaneous rotation angle based on the current state of the satellite:

$$\theta_j = \theta_j|_{\psi_j=0} - (2<e_j> + \gamma_j)\sin M_j \tag{11}$$

where γ_j denotes the amplitude of the once-*per*-orbit forced libration $\gamma_{,j}(t)$. In the evaluation of this model, the mean anomaly M is computed based on an unperturbed (constant mean motion n) orbit. This approach simplifies the rotational dynamics significantly compared to the actual behaviour. However, it allows us to gain insight into the first-order observability of rotational dynamics on the orbits of the moons of Jupiter, on a time scale and accuracy that is relevant for JUICE. However, even this first-order forced libration is expected to be very small for the Galilean moons (Comstock and Bills, 2003).

Although the obliquities of the Galilean satellites contain crucial information on their interior (Bills, 2005), it was found by Lainey et al. (2004b) that the orientation of the rotation axis of the Galilean satellites will have an influence on their positions of <1 km over a period of even 100 years. Consequently, we fix the orientation of the rotation axes of the Galilean satellites (w.r.t. the instantaneous equatorial plane of Jupiter) to the values provided by Archinal et al. (2011).

For the rotation model of Jupiter, we use the full *a priori* model from Archinal et al. (2011). It is expected that data from the Juno spacecraft will be used to improve the Jovian rotation model before JUICE's arrival in the system (Le Maistre et al., 2016).

2.3. Tidal models

The tidal interaction between Jupiter and the Jovian moons has a crucial influence on their long-term dynamics (Yoder and Peale, 1981; Greenberg, 1987; Malhotra, 1991; Peale and Lee, 2002). Most importantly, tidal interaction between the moons and Jupiter results in dissipation in their interiors, which has a secular influence on the semi-major axis, eccentricity and inclination of the moons.

Here, we model the influence of tides by their influence on the bodies' spherical harmonic coefficients, which we denoted as ΔC_{lm} and

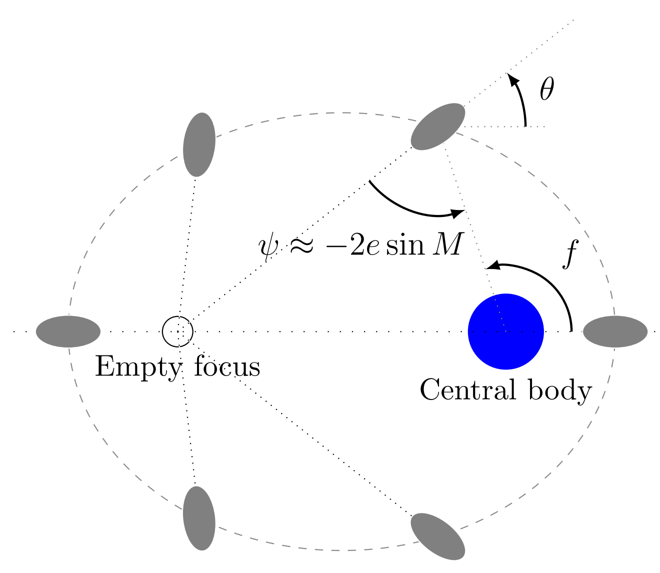

Fig. 1. Schematic planar representation of the non-librating ($\gamma'(t) = 0$) rotation of a tidally locked satellite on an eccentric orbit. Indicated are the true anomaly f, the body rotation angle θ and the instantaneous rotational offset angle ψ. Note that $\omega = 0$ in this figure, and Ω is undefined in the planar case.

ΔS_{lm} in Eq. (5). This approach automatically includes the influence of a given tide on the dynamics of all bodies when applying our model outlined in Section 2.1.

We distinguish three types of tides:

- Tides raised on Jupiter by the moons.
- Tides raised on the moons by Jupiter.
- Tides raised on the moons by other moons.

To determine the influence of the tides in a general fashion, we start from the expansion formalized by Kaula (1964), in which the tide-raising potential of body k at the position of body j is decomposed into spherical harmonics and expanded in orbital elements. Using this tide-raising potential, we compute the tidal correction to the values of $\Delta(C, S)_{lm}^{(i,j)}(t)$ for the leading order tidal modes. The influence of the tides raised on body j by body k is parameterized by the $(k_2)^{(j,k)}$ Love number and the $(k_2/Q)^{(j,k)}$ ratio, where Q denotes the body's quality factor. We model both these parameters independently for each combination of j and k, to assess the possibility to observe their frequency-dependence. To be able to apply the Kaula theory, we calculate the influence of the spherical harmonic corrections for the unperturbed (Keppler) orbit and then apply these to the corresponding actual orbit, in a manner that causes the tidal bulge to be raised consistently with the model described here. We have validated our model against existing literature results and obtain the correct secular tidal influence of the orbits of the satellites for the full Galilean system, both in the case where only a tide raised on a satellite is included (Lainey and Tobie, 2005) and where the tide raised on both the satellites and Jupiter are included (Lainey et al., 2009).

By using this model, we include the direct influence on the dynamics of body i of the tidal bulge raised on body j due to body k. This additional effect is not expected to have a secular influence on the semi-major axis, eccentricity or inclination of body i (as opposed to the indirect effect), but may be relevant for data analysis of the JUICE mission. We note that the models of (e.g., Efroimsky and Lainey, 2007) could also be used to include the physical effects that we consider here. The approach we use has the advantage of not requiring the use of 'fictitious' satellites (e.g., Mignard, 1980), instead modifying the (gravity field) properties of the satellites from their present state. However, the two-step implementation makes its implementation somewhat cumbersome.

For a future, more detailed analysis, of tidal effects on satellite dynamics the methodology recently developed by Boué et al. (2016) could be used, in which the tidal perturbation to the gravity field coefficients is treated as additional entries in the state vector, for which the differential equation is solved simultaneously with the orbital and rotational dynamics. Such an approach would be at the expense of increased model and computational complexity, but would ensure the internal consistency of the tidal model with the rotational and orbital dynamics.

2.4. Physical characteristics of the Galilean moons

In this section, we review the current observational state-of-the-art in the determination of the Jovian system's characteristics, as well as the expected near-term improvements in these models. We also discuss relevant improvements that JUICE orbit/flyby Doppler tracking data will produce, independently from the ephemeris generation.

The gravity fields of the Galilean moons have been estimated using flyby data from the Galileo spacecraft (Schubert et al., 2004). However, the J_2 and C_{22} could only be independently estimated for Io, due to the flyby geometry. For the other moons, hydrostatic equilibrium was assumed in the data analysis. Initially, the postfit residuals indicate that Ganymede possesses significant mass anomalies beyond spherical harmonic degree 2 (Anderson et al., 2004). Reanalysis of the data by Jacobson (2013) found, however, that this signature could be fully attributed to noise in the tracking data, originating from the Io plasma torus. We note that for JUICE, the dual-band tracking system will allow plasma noise to be removed from the data. Although no independent degree 3 gravity field coefficients are known for the Galilean moons, using Titan as an analogue indicates that they are of on the order of 10^{-6} (Iess et al., 2012).

The proposed Europa Multiple-Flyby Mission, will be able to provide an independent improved estimation of the degree 2 and 3 gravity field coefficients of Europa (Mazarico et al., 2015). For Europa, the JUICE flybys will allow the independent determination of the J_2 and C_{22} coefficients, while Callisto's full gravity field will be estimated up to at least degree 3 (Parisi et al., 2014). Orbiter tracking data of JUICE at Ganymede will allow the determination of its gravity field with high accuracy up to at least degree and order 12 (Titov et al., 2014).

The only Jovian moon for which any tidal characteristic has been observationally constrained is Io, for which Lainey et al. (2009) estimated the k_2/Q at 0.015 ± 0.003. This estimation was performed concurrently with that of Jupiter, which was determined to be $k_2/Q = (1.102 \pm 0.203)\cdot 10^{-5}$. Including the tracking data from the Galileo mission in the determination of tidal dissipation has thus far proven yielded negative results (Jacobson and Folkner, 2014). Doppler tracking data of the JUICE spacecraft will allow the independent determination of both the real and imaginary part of Ganymede's k_2 Love number, and the real part of Callisto's Love number (Parisi et al., 2014). Furthermore, EMFM tracking data will allow the determination of at least the magnitude of Europa's k_2 Love number (Mazarico et al., 2015; Park et al., 2015). Rereduction of astrometric data using the Gaia catalogue (Arlot et al., 2012) will likely improve the estimate of tidal dissipation before the JUICE mission, as it will improve the quality of part of the historic astrometric observations (see Section 4.3).

The frequency dependence of the quality factor Q of solar system bodies is poorly constrained at present. However, this dependency for both the moons and Jupiter can have a substantial effect on the long-term orbital evolution of the system, as shown by for instance Efroimsky and Lainey (2007) and Auclair-Desrotour et al. (2014). Our sensitivity analysis will include a separate analysis of k_2/Q at each of the forcing frequencies.

Librations of the Galilean moons are thus far unconstrained by observations, but extensive work has been carried out on modelling the influence of their interior structure on these moons' rotational dynamics (e.g. Rambaux et al., 2011; Van Hoolst et al., 2013). However, the influence of the libration on the dynamics stems from the libration of the entire body, as opposed to the shell libration alone, which is the focus of most analyses. Comstock and Bills (2003) analyzed the forced libration amplitude of the Galilean moons, assuming them to be rigid, and obtained amplitudes in the range of 10^{-4} (for Io) down to $5\cdot 10^{-6}$ (for Ganymede and Callisto). JUICE data from the GALA, JANUS and 3GM instruments will be used to constrain the once-*per*-orbit libration of Ganymede.

We use the nominal values for physical properties of Jupiter (gravity field; rotation) given by Campbell and Synnott (1985). These values correspond to within the error bounds to the later analysis by Jacobson (2001). We note that we have verified that changing the nominal values of the Jovian gravity field has a negligible impact on the results that we obtain for the pre- and postfit residuals. Substantial improvements in our knowledge of the Jovian gravity field are expected from the Juno mission, as analyzed in detail by Finnocchiaro (2012) and Le Maistre et al. (2016), respectively. Here, we will take a conservative approach and not assume in our nominal model the improvements in Jupiter gravity fields that Juno will provide. Nevertheless, we will discuss the influence of the great reduction in gravity field uncertainty that Juno will provide, thereby highlighting a further synergy between the two missions.

3. Sensitivity analysis

Here, we describe the details of the methods with which we perform sensitivity analysis of the dynamics of the Galilean moons. We start in Section 3.1 by listing the parameters for which we investigate the sensitivity of the dynamics. Subsequently, we describe our approach for obtaining realistic sensitivities of the Galilean moons' dynamics to the present uncertainty of these parameters in Section 3.2. Finally, we discuss the expected level of observability (for JUICE) of the dynamics of the Galilean moons in Section 3.3.

3.1. Simulation settings

We consider the following set of physical parameters and uncertainties of the Jovian system in our sensitivity analysis:

- Initial states of Jupiter, as well as Amalthea, Thebe and Himalia. We use an uncertainty in the ephemerides of the minor moons of 300 km (Christou et al., 2010; Emelyanov and Arlot, 2008). The uncertainty of the Jupiter ephemeris is estimated at about 10–40 km in right ascension α and declination δ, and about 1–5 km in range (Folkner, 2011; Fienga et al., 2014). However, these estimates are based on the inter-comparison between different ephemerides, and may very well be too optimistic an estimate for the true error: we use an uncertainty of 10 km in range and 100 km in α and δ.
- Static spherical harmonic coefficients for gravity fields of the Galilean satellites, up to degree and order 3, $C^i_{0,lm}$ and $S^i_{0,lm}$ for l=2,3, $m = 0\ldots l$ ($m = 1\ldots l$ for S coefficients), i=1..4. We use an uncertainty of 5 times the formal errors σ_F of the coefficients given by Schubert et al. (2004), and $5\cdot10^{-6}$ for the remaining coefficients, using the results of Iess et al. (2012) for Titan as a guideline.
- Full static spherical harmonic coefficients for gravity field of Jupiter, up to degree and order 4, $C^0_{0,lm}$ and $S^0_{0,lm}$ for l=2,4, $m = 0\ldots l$ ($m = 1\ldots l$ for S coefficients); zonal gravity field coefficients $C^0_{0,l0}$ up to degree 12. We use an uncertainty of 5 times the formal error σ_F of the coefficients given by Jacobson (2001), and 10^{-6} for the remaining coefficients.
- Longitudinal rotation amplitude (at orbital frequency) of each Galilean moon ψ_i. We use the ψ_i from Eq. (with zero $\gamma_{\prime i}$) in our nominal model. Since the addition of $\gamma_{\prime j}$ in Eq. (11) merely changes the amplitude of the once-*per*-orbit rotational variation in our model, but not the time-behaviour, we can directly use our results to assess the dynamics' sensitivity to the once-*per*-orbit libration $\gamma_{\prime i}$.
- Complex tidal Love number of each of the Galilean satellites and Jupiter, separately at each of the first-order forcing frequencies from each of these bodies $k_2^{(j,k)}$, with $j = 0\ldots4$, $k = 0\ldots4$, $j \neq k$. Both the static Love numbers $|k_2|$ and the dissipation parameters $k_2/Q\,(=\mathrm{Im}(k_2))$ are poorly constrained for the moons. We set $k_2 = 0.3$ for each of the moons, and $k_2/Q = 0.015$ (equal to Io's value provided by Lainey et al. (2009)). Although these values may be substantially different than the actual properties of the moons, the sensitivity scales linearly with their values (assuming their effect on the moons' orbits is small) and we discuss the influence of their actual value on their observability in Section 4.3 (if applicable). For Jupiter, $|k_2|$ and k_2/Q are set at nominal values of 0.38 and $1.1\cdot10^{-5}$, respectively.
- Gravitational parameters of Galilean satellites μ_i, $i = 1\ldots4$, as well as of the minor moons Amalthea, Thebe and Himalia: μ_5, μ_6 and μ_7, respectively. For the Galilean moons, we use 5 times the formal uncertainties σ_F given by Schubert et al. (2004). The uncertainties in the masses of Amalthea and Himalia are taken from Anderson et al. (2005) and Emelyanov (2005), respectively. No direct determination of the mass of Thebe is available, so its uncertainty is set at 100% of its nominal value, which is derived from observations of its size and assumptions of its composition.

Table 1
Nominal values $p_i^{(0)}$ and perturbations $(p_i^{(\Delta)} - p_i^{(0)})$ of parameters under consideration, with perturbed parameters denoted as $p_i^{(0)}$.

Parameter	Nominal value $p_i^{(0)}$	Perturbation $p_i^{(\Delta)} - p_i^{(0)}$
$\Delta\mathbf{x}_0(t_0)$	0 km	10 km (range)/100 km (α/δ)
$\Delta\mathbf{x}_{5..7}(t_0)$	0 km	300 km (each component)
$(C,S)^{1..4}_{0,20}$; $(C,S)^{1..4}_{0,22}$	Values from Schubert et al. (2004)	$5\sigma_F$ from Schubert et al. (2004)
$(C,S)^{1..4}_{0,21}$; $(C,S)^{1..4}_{0,3m}$ m=0..3	0	10^{-6}
$J^0_{0,2;3;4;6}$; $(C,S)^{1..4}_{0,22}$	Values from Jacobson (2001)	5 σ_F from Jacobson (2001)
$J^0_{0,5;7..12}$; $(C,S)^0_{0,21}$; $(C,S)^0_{0,lm}$ l=3..4, $m \leq l$	0	10^{-6}
$\lvert k_2\rvert^{0,k}$, k=1..4	0	0.38
$\lvert k_2\rvert^{j,k}$, j=1..4, k=0..4, $j \neq k$	0	0.3
$(\lvert k_2\rvert/Q)^{0,1..4}$	0	$1.1\cdot10^{-5}$
$(\lvert k_2\rvert/Q)^{j,k}$ j=1..4, k=0..4, $j \neq k$	0	0.015
$\psi_{1..4}$	0 rad	$2\langle e_{1..4}\rangle \sin M_{1..4}$ rad (note that $\gamma_{1..4}' = 0$)
$\mu_{1..4}$	Values from Schubert et al. (2004)	$5\sigma_F$ from Schubert et al. (2004)
μ_5	$1.3\cdot10^8$ m^3 s^{-2}	$2.9\cdot10^7$ m^3 s^{-2}
μ_6	$2.7\cdot10^7$ m^3 s^{-2}	$2.7\cdot10^7$ m^3 s^{-2}
μ_7	$2.8\cdot10^8$ m^3 s^{-2}	$4.0\cdot10^7$ m^3 s^{-2}

We summarize the nominal and perturbed values of the parameters that we consider, denoted $p_i^{(0)}$ and $p_i^{(\Delta)}$, respectively, in Table 1. Since the uncertainties in the parameters that we consider are small, their effect on the orbital dynamics is effectively linear. Therefore, modifying the uncertainty of any of the parameters by a factor α will scale both the pre- and postfit residuals by the same factor α, making the results we present easily generalized to other values of $(p_i^{(\Delta)} - p_i^{(0)})$.

In our analysis we do not analyze the effect of the inclusion of relativistic effects on the orbits, as these effects can be modelled to an accuracy that is more than sufficient for the purposes of the JUICE mission. Although it may very well be necessary to include the (first-order) relativistic corrections, no additional parameters will need to be added to the estimation, and conversely there is no risk of uncertainties in physical parameters observably influencing the relativistic correction.

3.2. Orbit fitting

To determine the sensitivity of the orbits of the Galilean moons to the presence of heretofore unmodelled physical effects, as well as the present uncertainty in the characteristics of the Jovian system (as summarized in Table 1), we apply the method analogous to the one employed by e.g. Tragesser and Longuski (1999), Lainey and Tobie (2005), Iorio and Lainey (2005), Beauvalet et al. (2012), and discussed conceptually by Lainey (2016). In this section, we denote the full state vector of the Galilean moons by $\mathbf{x}$, which is a function of time t, and parameterized by the adjustable initial state vector $\mathbf{x}_0$ of the Galilean moons, as well as a parameter value p_i as:

$$\mathbf{x} = \mathbf{x}(t;\, \mathbf{x}_0,\, p_i) \tag{12}$$

Since we only consider the sensitivity to a single parameter p_i at a time, we only explicitly include a single parameter dependency in Eq. (12).

First, we generate what we term a prefit orbit-difference $\Delta\mathbf{x}_{pre}$. These are obtained by propagating the dynamics with a perturbations turned on (using $p_i^{(\Delta)}$), and then subtracting the dynamics with the perturbations turned off (using $p_i^{(0)}$), so that:

$$\Delta\mathbf{x}_{pre}(t) = \mathbf{x}(t;\, \mathbf{x}_0,\, p_i^{(\Delta)}) - \mathbf{x}(t;\, \mathbf{x}_0,\, p_i^{(0)}) \tag{13}$$

$$\approx\left(\frac{\partial \mathbf{x}}{\partial p_i}\right)(p_i^{(\Delta)} - p_i^{(0)}) \tag{14}$$

where the second step follows from linearization of the problem. Consequently, the prefit difference is simply obtained by propagating the sensitivity matrix $(\partial \mathbf{x}/\partial p_i)$, as discussed by e.g. Montenbruck and Gill (2000).

For the second step of the analysis, we simulate ideal three-dimensional measurements of the positions of the moons at regular intervals, using the perturbed dynamics $\mathbf{x}(\mathbf{x}_0, t; p_i^{(\Delta)})$. We create a measurement of the position of each of the moons every 4 h over a period of 5 years (somewhat longer than the nominal mission duration, see Section 1). Subsequently, we use these simulated observations to estimate the initial states of the moons, but now using $p_i^{(0)}$ as the parameter value of parameter i in our dynamical model.

We use a least-squares orbit determination algorithm (e.g. Montenbruck and Gill, 2000; Milani and Gronchi, 2010), in which we weigh each of the simulated observations equally. We do not adjust any model parameters, but *only* estimate the initial states of the four moons. The correction to the initial state vector $\mathbf{x}_0$ is obtained from

$$\min_{\Delta \mathbf{x}_0}\left(\sum_j \|\mathbf{x}(t_j;\, \mathbf{x}_0 + \Delta\mathbf{x}_0,\, p_i^{(0)}) - \mathbf{x}(t_j;\, \mathbf{x}_0,\, p_i^{(\Delta)})\|^2\right) \tag{15}$$

so that the least-squares adjustment uses the ideal three-dimensional measurements at the times t_j (calculated as $\mathbf{x}(t_j;\, \mathbf{x}_0,\, p_i^{(\Delta)})$) to find $\Delta\mathbf{x}_0$. Consequently, the postfit orbit difference then becomes:

$$\Delta\mathbf{x}_{post}(t) = \mathbf{x}(t;\, \mathbf{x}_0 + \Delta\mathbf{x}_0,\, p_i^{(0)}) - \mathbf{x}(t;\, \mathbf{x}_0,\, p_i^{(0)}) \tag{16}$$

As a result, the methodology that we use includes the capabilities of the nominal dynamical model to absorb the uncertainties and unmodelled effects listed in Section 3.1. For an effect that can be largely absorbed by the initial states in this manner, concurrently estimating it with the state would result in a (near-)complete correlation between the estimates of the two. We stress that our approach is designed to analyze the influence of a *single* parameter at a time, and we do not examine the possibility of multiple parameters potentially being manifested in the dynamics in a similar manner, leading to correlated estimates in the data analysis. Such correlations would depend strongly on the specific types, quality and cadence of tracking data this is used, which is beyond the scope of this paper. As such, we provide an upper bound of the effects that could be observably manifested in the data.

This capability to absorb unmodelled effects is especially strong for physical parameters for which the influence on the dynamics is largely manifested as a constant change in mean motion, node and periapsis frequency of the satellite. The influence of any such parameters can, to first order, be mimicked by a small change in the satellites' semi-major axes (Lainey et al., 2004b). Although the influence of tidal dissipation, which causes a secular change in the mean motion *rate*, can be partly absorbed by the initial states (Lainey and Tobie, 2005), this absorption is much less efficient.

Due to the high accuracy of the measurements performed by JUICE, it is important to determine whether higher-order effects of the parameters in Table 1 (which may not present themselves as absorbable influence on the dynamics, will be observable). The primary contribution of this article is the detailed analysis of the observable influence of the set of parameters listed in Table 1, with a focus on the influence over a short period of time (5 years), but considering a much smaller signature to be observable than has so far been considered (20 m; see Section 3.3). This is in contrast to previous analyses by e.g., Lainey et al. (2004b) and Iorio and Lainey (2005), who considered the dynamical behaviour over a longer time period (~100 years), but with a much lower required accuracy (typically >100 km).

3.3. Observability of physical effects

In interpreting the results of the simulations, we will compare the behaviour of the postfit residual with the expected accuracy of the measurements of the positions of the moons that JUICE will provide. This measurement accuracy is a combination of the uncertainty in both the observations and the estimation of the position of JUICE w.r.t. the body under consideration (e.g. Lainey et al., 2007; Hees et al., 2014).

The detailed analysis of the inversion of the JUICE tracking data for ephemeris generation is beyond the scope of this article (Section 1). Instead, this section provides initial estimates for the uncertainty in the dynamics of the moons that can be obtained, using previous analyses of the JUICE mission and experience with, e.g. Cassini. These estimates will be used in Section 4 to assess the possibility that the parameters listed in Table 1 will need to be adjusted during the ephemeris generation from JUICE data.

During the Ganymede spherical orbit phase at 500 km altitude, the spacecraft orbit is to be determined w.r.t. Ganymede with an uncertainty in the order of 1 m (Titov et al., 2014). It is found by Parisi et al. (2012) that this accuracy will be attainable for the radial and cross-track direction, but that an error up to 10 m could occur for the along-track direction. During the flybys of the satellites, the expected/required positional uncertainty is not as clearly defined. However, experience with Cassini flybys at Titan show that the orbit can be reconstructed with an accuracy of about 10 m (in plane) to 100 m (out-of-plane) (Antreasian et al., 2008).

The use of the dual-frequency (X- and Ka-band) radio tracking system for 3GM (see Section 1) will allow range measurements with an uncertainty of <20 cm to be obtained for all but the smallest solar separation angles, since the solar plasma noise is cancelled by this system. The quality of the Doppler data will be <0.01 mm/s at 60 s integration time (Iess, 2013). By comparison, tracking data from missions such as Cassini and Rosetta (which rely on an X-band signal only) show a clear impact of the solar angle (Iess et al., 2014), with a mean performance close to an order of magnitude worse than that required for JUICE. Present uncertainty in VLBI data is at the 1.0 nrad level (Duev et al., 2012; Jones et al., 2015), using an X-band signal. The use of the Ka-band signal could in principle result in VLBI observables that are 3–4 times more precise (Curkendall and Border, 2013). While the use of Ka-band in VLBI is at present relatively uncommon (Majid and Bagri, 2008), a steady progress towards routine use of this advanced VLBI option is underway (Horiuchi et al., 2013; Malkin et al., 2015).

Based on this comparison, we estimate that the combined 3GM and PRIDE observations will allow the position to be constrained to a precision and accuracy that is several times better than that of Cassini. However, the results of the sensitivity analysis (Section 4) are presented in a general fashion, allowing them to be applied for a wide range of spacecraft orbital positioning accuracies.

The generation of the ephemerides of the moons from the tracking data will be performed in a dynamical manner (e.g., Montenbruck and Gill, 2000). This will allow the PRIDE and 3GM data to be fused in a general fashion, without the requirement that both experiments be performed simultaneously. Concurrent measurements of both range and angular position would allow the three-dimensional position of the spacecraft to be determined kinematically, however, without any need for a dynamical model to link the observations at different epochs. Such an approach could be advantageous in stabilizing the numerical estimation problem of the ephemeris generation.

The orbit phase of JUICE around Ganymede is comparatively short (9 months; 5 months elliptical and high altitude, 4 months circular at 500 km altitude). Especially the circular orbit phase will provide highly accurate constraints on the position of Ganymede, as the spacecraft orbit determination error will be smallest in this phase. Due to the short duration, however, it will be extremely challenging to use the tracking data during Ganymede orbit to identify and decorrelate the dynamical signature of the physical parameters under investigation, at least in terms of their influence on the dynamics of the Jovian system as a whole. Nevertheless, these data will be highly useful to constrain the dynamics of Ganymede, and provide an accurate ‘ground truth’. In general, we will consider a postfit signature on the dynamics of Ganymede that has an r.m.s. magnitude of about 20 m to be potentially observable from JUICE data alone. We will, when applicable, discuss parameters for which postfit residual behaviour below this level, especially during the orbit phase, may be observable.

Although JUICE will perform 2 flybys of Europa, these flybys are separated in time by only about ~2 weeks. Consequently, these flyby data will not allow any signatures that build up over the full mission duration of 3.5 years to be directly observed. However, Europa's position will influence the motion Ganymede, allowing the tracking of JUICE at Ganymede to be used as input for the Europa ephemeris. Furthermore, JANUS observations of Europa and Io will be used to supplement the input to the ephemeris generation procedure (Section 1). This provides the possibility to improve Europa's ephemeris well beyond the current state-of-the-art, but not to the same level as that of Ganymede. Here, we use a rough guideline of 200 m as the level of observable perturbation of Europa.

The dynamics of Io will not be directly constrained by radio tracking data (although its indirect influence on the other moons will be visible). As such, the JUICE-derived Io ephemeris will likely be of substantially lower quality ($\gtrsim$1 km) than that of the other moons, and we do not discuss the pre- or postfit residuals for Io in most cases.

The many (~10) flybys of Callisto will allow this moon's ephemeris to be constrained very well, although not at the same level as that of Ganymede, as the spacecraft orbit uncertainty will be higher during the flybys than during the orbit. Moreover, due to Callisto's relatively distant orbit, the signature of physical parameters on its orbit will be quite small. We put the limit of observable signature on Callisto's orbit at 50 m.

4. Results and discussion

In this section, we present the results of our sensitivity analysis of the dynamics of the Galilean moons, for the parameters listed in Section 3.1, using the approach discussed in Section 3.2. We will focus on the sensitivity of the dynamics of Ganymede, as JUICE tracking data will be most dense and accurate for this body (Grasset et al., 2013), and its dynamics will consequently be constrained to the highest accuracy (Section 3.3). Where relevant, we will also discuss the influence on the dynamics of the Europa, Callisto and Io.

We start by discussing the sensitivity of the Galilean moons' dynamics to a change in the dynamics of the minor moon, as well as Jupiter, in Section 4.1. Subsequently, we discuss the sensitivity to the static gravity field coefficients, tidal characteristics and rotational characteristics under consideration (Table 1) in Sections 4.2–4.4, respectively.

4.1. Positions

In Fig. 2, we show the prefit sensitivity of the Jupiter-centered positions of the Galilean satellites to the barycentric position of Jupiter, see Eq. (13). These sensitivities are purely a result of the external bodies' third-body perturbations being slightly modified due to a change in position of the entire Jovian system. It is clear that the sensitivity of the Galilean satellites' orbits to Jupiter's position is quite weak, on the order 10^{-5} m/m for the inner three moons. The strongest sensitivity (up to $2.5\cdot10^{-4}$ m/m) is observed for Callisto, where the external third-body perturbations will be strongest. The results from Fig. 2 show that even a 100 km positional error of Jupiter (Table 1) will result in a prefit error of only 30 m for Callisto and 2.5 m for Ganymede. In our postfit analysis, we have found that the influence of the Jovian ephemeris on the postfit residual is negligible, even if the present estimates of the uncertainty in Jupiter's ephemeris are too optimistic by an order of magnitude.

Although the Jovian position is not significantly influential on the Jupiter-centered position of the satellites, Earth-based lateral position (PRIDE) and range (3GM) observations will be directly influenced by the barycentric position uncertainties of Jupiter. This will degrade the realistic weights that should be applied to Earth-based range and lateral position measurements of the moons. The estimation of measurement biases would be advisable, to improve the weighting of the Earth-based observations (as well as remove any unrelated systematic uncertainties in the measurements). Whether the Jupiter initial state will need to be estimated concurrently with that of the moons will depend on the correlation between the Jupiter and moon initial states that is obtained during the tracking data inversion. In particular, if the correlation is sufficiently high that the signature of Jupiter's dynamics that ‘leaks’ into the satellite dynamics approaches some threshold (which we set to 20 m and 50 m here for Ganymede and Callisto, respectively; Section 3.3), the concurrent estimation is required.

Conversely, we find a prefit sensitivity of the barycentric position of Jupiter to the initial Jupiter-centered positions of the Galilean satellites at the level of 1 m/m. Considering the present uncertainty in the Galilean moons' positions, using *a priori* moon ephemerides for the construction of a new Jovian ephemeris from JUICE data may introduce an error that is well above the formal uncertainty in the Jupiter ephemeris. This effect is especially likely due to the presence of the moons' once-*per*-moon-orbit influence on Jupiter's dynamics, which will not be strongly absorbable by Jupiter's barycentric motion. Consequently, it is recommended that the Jovian ephemeris be computed either concurrently with, or following, the generation of the Galilean moon ephemerides.

We find that postfit residuals of the simulations with perturbed

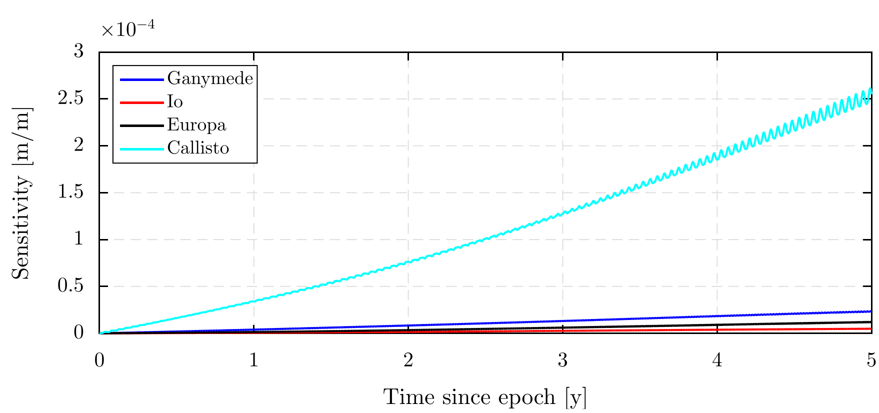

Fig. 2. Norm of sensitivity of Galilean satellite position w.r.t. initial Jupiter position, $|\partial\mathbf{r}_i(t)/\partial\mathbf{r}_0(t_0)|$.

initial state of the small Jovian moons Amalthea, Thebe and Himalia are all at the sub-m level, despite the large uncertainty in the linear positions of these moons, which is at hundreds of km (Table 1). Therefore, using *a priori* ephemerides of the minor moons will not degrade the Galilean moons' ephemeris generation. Nevertheless, astrometric observations of the inner moons obtained using the JANUS instrument might allow for valuable independent determinations of tidal effects in the Jovian system (Lainey and van Hoolst, 2009).

4.2. Gravity fields

As discussed in Section 2.4, the gravity fields of the outer three Galilean moons will be improved significantly using the Doppler tracking data from JUICE during flybys/orbit. Nevertheless, it is important to analyze whether these improved gravity fields should be used during ephemeris generation, or whether the current fields may be used. Additionally, our results in this section will show whether the ephemerides could be used to obtain estimates of the moon gravity fields that are independent from the Doppler data.

The prefit residual of the sensitivity of the Galilean moons to the degree 2 gravity fields of the moons has been analyzed previously by Lainey et al. (2001). There, it is found that the complete prefit influence (as opposed to the 5σ influence we consider here, see Table 1) of the satellites' gravity fields amounts to as much as 50 km/year for Io. The influence of the uncertainty in the gravity field is substantially smaller, but still up to 500 m r.m.s. for Ganymede and 3 km and 5 km r.m.s. for Europa and Io, respectively (after 5 years). However, we find that the postfit r.m.s. residuals are largely at the sub-m level for the dynamics of all moons (with a single exception of 5 m for Io's sensitivity to its own C_{22}), as shown in Table 2. We find ratios of pre- and postfit residuals up to and above 1000. This was to be expected considering the fact that the influence of these coefficients is manifested almost entirely as a slight increase in these moons' semi-major axes, see Section 3.2; Lainey et al. (2004b).

These results unambiguously show that the gravity fields of the Galilean moons may be taken at their *a priori* values during ephemeris generation from JUICE data. Conversely, it will be impossible to obtain reliable estimates of these coefficients from the generation of the ephemerides.

The pre- and postfit residuals for simulations including the uncertainty in the gravitational parameters of the Galilean moons are given in Table 3. Again, it can be seen that the influence of these parameters is very effectively absorbed by the states of the moons, although postfit residuals at the 10–100 m remain for the inner three moons. This is a result of the direct interaction between the moons, as opposed to the influence between Jupiter and the moons, which is easily absorbed into the nominal dynamics (Section 3.2). The given postfit residuals in Table 3 show that the current level of uncertainty in the moons' masses will be observable in the JUICE-derived ephemerides of the moons. In particular, a 32.5 m postfit signature in the orbit of Ganymede, as a result of μ_2, is well above the estimated observability floor of 20 m, (Section 3.3). The present uncertainty in μ_3 may, at 100 m postfit residual be weakly visible in the dynamics of Europa.

However, flybys of Europa by JUICE, as well as possibly by EMFM, will improve μ_2 to a level where its uncertainty will be inconsequential for ephemeris generation of Ganymede (requiring only a modest improvement of μ_2 uncertainty of a factor ~2). Similarly, the uncertainty of μ_3 will be greatly reduced by 3GM/PRIDE Doppler tracking during both the flybys and orbit phase of Ganymede, reducing the influence of its uncertainty on the dynamics (which is highest for Europa at 100 m). The influence of the current uncertainty in μ_1 is below observable levels (Section 3.3) for the dynamics of Ganymede (<1 m), and for Europa as well (<40 m).

We show the pre- and postfit residuals for the simulations with the uncertainty in the zonal gravity field coefficients of Jupiter in Table 4. We found postfit residuals of <1 m in the orbit of Ganymede for each of the non-zonal coefficients. The even zonal coefficients influence the prefit orbits of the moons much more strongly than the odd coefficients (up to 20, 150 and 250 km for the J_2 influence on Ganymede, Europa and Io, respectively). However, this influence of the even coefficients is very efficiently absorbed into the initial states of the moons. In particular, the postfit influence of $J_{0,2}^{(0)}$ is largest for Europa at 125 m, with a signature of 25 m for Ganymede, at the limit of observability. For the odd zonal coefficients, however, the absorption is very limited, with significant postfit influence of both J_3 and J_5 (45 m and 85 m influence for Ganymede, respectively; ≈250 m influence for Europa from both coefficients).

However, the numerical simulations from Finnocchiaro (2012) show that the J_2–J_5 of Jupiter will be estimated with a formal error of $\sim10^{-10}$ from Juno data, which is 3–4 orders of magnitude more accurate than the uncertainties presented by Jacobson (2001), which we use here (see Table 1). As a result, we can conclude that the post-Juno Jovian gravity field will be sufficiently accurate to result in a postfit influence on the Galilean satellites orbits that is ≪1 m over a period of 5 years, even when scaling up the formal error that Finnocchiaro (2012) obtain by more than an order of magnitude. However, if the gravity field of Jupiter is not improved beyond the current state-of-the-art (i.e if Juno fails to deliver Jovian gravity fields), Jovian zonal gravity field coefficients (of degree 2, 3 and 5) will have to be estimated concurrently with the ephemerides created from JUICE data. The situation may be alleviated somewhat by the sensitivity of the JUICE spacecraft itself to the Jovian gravity field.

4.3. Tidal properties

The r.m.s. of the pre- and postfit residuals of the simulations incorporating the tidal properties of both Jupiter and the Galilean

Table 2
Pre- and post fit r.m.s. position residuals for Galilean moon degree 2 gravity field coefficients (only residuals >0.1 m shown).

	r.m.s. prefit residuals [m]				r.m.s. postfit residuals [m]			
	Io	**Europa**	**Ganymede**	**Callisto**	**Io**	**Europa**	**Ganymede**	**Callisto**
$C_{0,20}^{(1)}$	3128.89	1753.43	215.62	0.16	0.75	0.20	–	–
$C_{0,22}^{(1)}$	5630.38	3136.88	354.28	0.28	4.85	0.89	0.21	–
$C_{0,20}^{(2)}$	77.52	59.41	37.37	–	–	0.15	–	–
$C_{0,22}^{(2)}$	139.16	106.77	67.38	–	–	0.29	–	–
$C_{0,20}^{(3)}$	24.25	92.74	228.18	–	–	–	0.21	–
$C_{0,22}^{(3)}$	43.13	164.66	405.03	–	–	0.20	1.01	–
$C_{0,20}^{(4)}$	–	–	–	14.71	–	–	–	–
$C_{0,22}^{(4)}$	–	–	–	33.07	–	–	–	0.35

Table 3
Pre- and post fit r.m.s. position residuals for Galilean moon gravitational parameters (only residuals >0.1 m shown).

	r.m.s. prefit residuals [m]				r.m.s. postfit residuals [m]			
	Io	**Europa**	**Ganymede**	**Callisto**	**Io**	**Europa**	**Ganymede**	**Callisto**
μ_1	1983.35	450.35	2792.56	5221.64	0.59	34.01	0.86	0.63
μ_2	781.41	2880.70	3941.54	1585.21	84.78	6.29	32.50	0.89
μ_3	1672.91	1443.05	1630.08	917.34	1.88	109.45	2.62	3.40
μ_4	21.60	47.64	132.46	588.24	–	–	2.05	0.25

Table 4
Pre- and post fit r.m.s. position residuals for Jupiter zonal gravity field coefficients (only residuals >0.1 m shown).

	r.m.s. prefit residuals [m]				r.m.s. postfit residuals [m]			
	Io	**Europa**	**Ganymede**	**Callisto**	**Io**	**Europa**	**Ganymede**	**Callisto**
$J_{0,2}^{(0)}$	253,634.73	148,666.39	19,696.71	6447.27	65.89	127.54	25.60	19.46
$J_{0,3}^{(0)}$	188.44	421.60	169.78	10.10	83.52	269.64	83.57	3.38
$J_{0,4}^{(0)}$	75,883.73	42,357.64	2350.35	101.40	40.98	32.82	3.49	0.63
$J_{0,5}^{(0)}$	114.12	305.71	78.28	0.49	91.62	229.43	44.11	0.38
$J_{0,6}^{(0)}$	8865.84	4927.96	474.49	0.75	7.34	2.79	0.40	–
$J_{0,7}^{(0)}$	6.43	15.02	1.90	–	5.50	11.74	1.60	–

satellites are shown in Table 5. In this table, we only show the interaction between Jupiter and the satellites, omitting the results for the tides raised between the Galilean satellites (discussed below). We explicitly show the time-behaviour of the pre- and postfit behaviour for the dynamics of Ganymede due to the tides raised by and on Io and Europa in Fig. 3.

As discussed in Section 3.2, the initial states of the moons are unable to strongly absorb the signatures of tidal dissipation. From Table 5, it is clear that when considering the dynamics of the inner three satellites, the influence of the tidal dissipation is dominated by the interaction of Jupiter with Io (maximum r.m.s. postfit residual of 100–250 m for the inner three moons), whereas the influence of the tidal interactions with Europa and Ganymede are considerably weaker (up to only 20 m and 0.5 m, respectively).

Assuming 0.015 as a nominal value for Io's dissipation parameter $(k_2/Q)^{(1,0)}$ (Table 1), its observable r.m.s. postfit influence on Ganymede's position is about 120 m over 5 years, and correspondingly (with a factor of approximately $(3.5/5)^2 \approx 0.5$) smaller over the nominal mission duration of 3.5 years. Considering the quality of the tracking data and orbit reconstruction (on the order of 20 m on average; see Section 3.3), this means that JUICE will likely be able to observe Io's internal dissipation (at Jupiter's forcing frequency) independently from the estimate obtained by Lainey et al. (2009) using astrometric data.

The total influence of Jupiter's tidal dissipation due to the Io-raised tide ($(k_2/Q)^{(0,1)} = 1.1 \cdot 10^{-5}$; see Table 1) on Ganymede is roughly a factor 5 smaller than that of Io's dissipation at about 25 m (see Table 5), with an observable postfit residual at the limit of observability. This is in contrast to the results found by Lainey et al. (2009), who obtain similar relative uncertainties for $k_2/Q)^{(0,1)}$ and $(k_2/Q)^{(1,0)}$. This is due to the significant imbalance in the uncertainties of the dynamics of Ganymede on the one hand (~20 m) and Io and Europa on the other hand (~200–1000 m) that JUICE tracking data will produce (Section 3.3). Due to the direct influence of the tide raised on Io on e_1 (Kaula, 1964), the signature of $(k_2/Q)^{(1,0)}$ is especially strong for Ganymede (Lainey and Tobie, 2005), compared to the influence of the tide raised on Jupiter. Consequently, Jupiter's internal dissipation will not be estimable from JUICE tracking data alone to a level that can be competitive with

Table 5
Pre- and post fit r.m.s. position residuals for tidal characteristics of Galilean moons and Jupiter (only residuals >0.1 m shown; nominal values for $k_2/Q^{i,0}$ all set to 0.015).

	r.m.s. prefit residuals [m]				r.m.s. postfit residuals [m]			
	Io	**Europa**	**Ganymede**	**Callisto**	**Io**	**Europa**	**Ganymede**	**Callisto**
$(k_2/Q)^{(0,1)}$	1139.07	502.37	60.72	–	202.18	73.47	23.49	–
$(k_2/Q)^{(0,2)}$	5.63	7.76	2.61	–	1.65	2.60	1.11	–
$(k_2/Q)^{(0,3)}$	0.28	0.94	2.97	–	–	0.12	0.51	–
$(k_2/Q)^{(0,4)}$	–	–	–	–	–	–	–	–
$(k_2/Q)^{(1,0)}$	1307.66	396.22	328.41	0.11	146.28	252.04	112.18	–
$(k_2/Q)^{(2,0)}$	68.23	22.65	10.69	–	13.65	20.54	10.47	–
$(k_2/Q)^{(3,0)}$	–	0.15	0.66	–	–	–	0.18	–
$(k_2/Q)^{(4,0)}$	43.32	15.79	46.45	0.26	–	–	–	0.14
$(k_2)^{(0,1)}$	19,922.90	11,457.65	803.29	117.47	11.81	15.81	0.79	0.42
$(k_2)^{(0,2)}$	2632.21	1502.81	244.89	16.33	18.81	2.21	0.34	–
$(k_2)^{(0,3)}$	376.44	917.89	915.69	15.43	0.32	4.71	0.50	–
$(k_2)^{(1,0)}$	802.77	1113.12	641.46	0.13	62.26	16.46	3.86	–
$(k_2)^{(2,0)}$	121.44	51.72	79.88	–	1.04	10.69	1.50	–
$(k_2)^{(3,0)}$	0.98	3.03	11.33	0.16	0.48	1.16	5.73	–

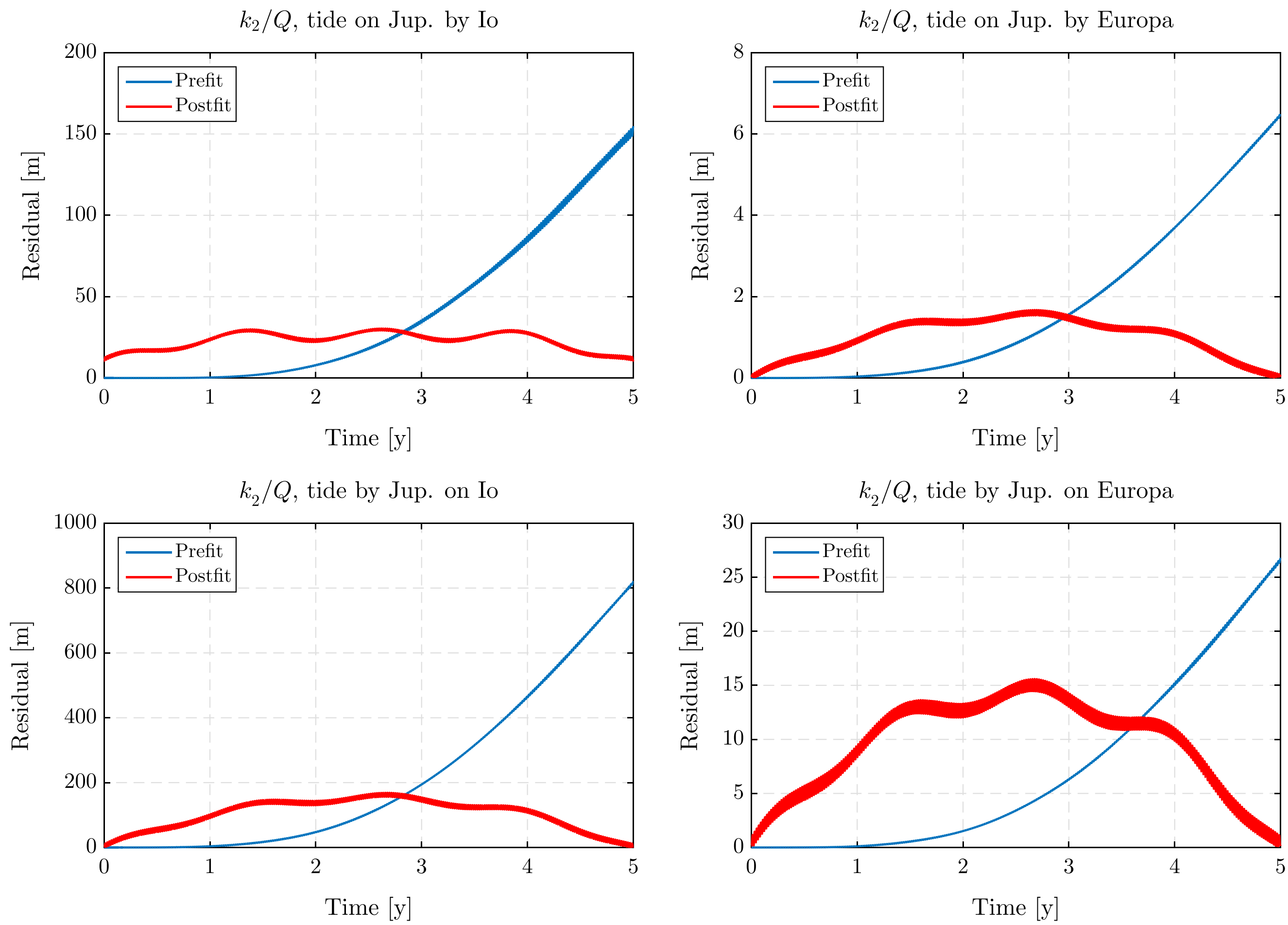

Fig. 3. Sensitivity of Ganymede's position to the degree 2 tidal dissipation of tides raised by Jupiter on Io/Europa and vice versa.

results from Earth-based astrometry.

The signature of the tidal dissipation on the orbits increases quadratically with time (e.g., Kaula, 1964). Comparing the measurement time of the astrometric observations (~120 years) with that of JUICE (3.5 years) shows that the signature is about 1200 times stronger when analyzing the astrometric data set. However, the observational accuracy of the astrometry is at about 50–450 km (Lainey et al., 2009), whereas the accuracy of the orbit reconstruction for the moons will be around 20 m for Ganymede (Section 3.3), a difference of a factor 2500. For the estimated observability limit of 200 m for Europa, this ratio drops to 250. However, the optical astrometry is equally distributed and equally accurate for the four Galilean moons, while the JUICE ephemeris solution will be much more accurate for Ganymede, complicating the estimation problem. The quantitative influence of this illposedness for the ephemeris generation and parameter estimation from JUICE data should be taken into account and analyzed when performing (simulations of) the tracking data inversion.

We also note that a reanalysis of existing astrometric data using the Gaia star catalogue will likely improve the existing constraints on Io's dissipation (see Section 2.4). It is estimated by Arlot et al. (2012) that rereducing the historical astrometric observations using the Gaia catalogue will result in a consistently improved accuracy of 10 mas, corresponding to a linear position uncertainty of the moons of 30 km. Future analyses will be dedicated to investigating the influence that this improvement in astrometric data will have on the estimate of the tidal dissipation.

For the influence of the tides shown in Fig. 3, the postfit behaviour in the dynamics of Ganymede for the tides involving Io and Europa is rather different from the typical behaviour. This typical behaviour, which we *do* observe when running our code with only a single moon, is parabolic (with part of the parabola mirrored on the abscissa since the residual is always positive), as discussed by Lainey (2016). The main reason for this difference is that the simulation results obtained here use three-dimensional observations of each of the moons that are weighted *equally* in the least-squares adjustment (Section 3.2). As a result, the estimation focuses on reducing the postfit residual in Io's orbit when considering $(k_2/Q)^{(1,0)}$, since this is where the influence on the dynamics is the greatest (Table 5). We indeed see there that the ratio of pre- to postfit residual is ≈10 for Io, whereas it is only about 3 for Ganymede, despite rather similar prefit behaviour. Although orbits of Ganymede most likely exist for which this ratio will be higher than 3, these orbits do not minimize the total residual of all moons in Eq. (15), and therefore the estimator does not converge to such dynamics.

This indicates an inherent incompatibility of the dynamical possibilities to absorb $(k_2/Q)^{(j,k)}$ into the dynamics of Ganymede on the one hand, and Io and Europa on the other hand. Therefore, the use of optical astrometric observations of Europa and Io (either from Earth or JANUS), combined with the tracking data analysis, will make a substantial difference in the degree to which the tidal signatures can be recovered. As a result, a combined analysis and planning optimization of the radio tracking and optical astrometric observations from JUICE will be crucial for robustly assessing the capabilities of the mission to contribute to constraining the tidal parameters.

The dissipation inside Europa could be visible in JUICE tracking data, with a signature of $(k_2/Q)^{(2,0)}$ that has an amplitude of about 15 m in the postfit residual of Ganymede over 5 years (see Table 5). However, recovering this signature from the ephemerides will require highly accurate spacecraft orbit reconstruction quality at the moons, particularly during the flybys. Furthermore, we see that the r.m.s. magnitude for both Europa's and Ganymede's orbit is very similar in both the pre- and postfit analysis for $(k_2/Q)^{(2,0)}$, highlighting the incompatibility of the moons' orbits to absorb its influence. Consequently, it is likely that the lack of highly accurate observations of Io by the JUICE mission will reduce the postfit sensitivity of Ganymede's (and Europa's) orbit to $(k_2/Q)^{(2,0)}$. We do note that we have set $(k_2/Q)^{(2,0)} = 0.015$ in our analysis. If JUICE cannot detect any signature of Europa's dissipation, it may be able to place a relatively weak upper bound on its magnitude.

As can be seen from Fig. 3, the pre- and postfit signatures of the dissipation parameters are quite similar in behaviour (although not in magnitude). As such, any estimate of the tidal parameters will be strongly correlated, at least if the determination is based (almost) exclusively on observations of the dynamics of Ganymede. Consequently, observations of multiple moons (optical astrometry and the Europa flybys) will be crucial to decorrelate the tidal signatures. Based on the magnitude of the signatures of the tides, however, the influence of all but the $(k_2/Q)^{(1,0)}$ will be very small. It may be possible that Jupiter's tidal properties will be independently determined by tracking-data analysis of the Juno spacecraft. This would provide great synergy between the two missions, as it would allow, for the first time, a strong decorrelation of the estimate of the dissipation inside Jupiter and Io.

For the dissipation inside Ganymede, the nominal postfit r.m.s. sensitivity of <1 m (even with the uniform weighting) means that $(k_2/Q)^{(3,0)}$ cannot be constrained to a value that cannot be excluded *a priori* from geophysical models. However, this parameter will be accurately determined from JUICE Doppler tracking data during the Ganymede orbit phase (Section 2.4).

Furthermore, we find no significant influence on the orbit of Callisto from any of the tides under consideration. Consequently, flybys of Callisto will not contribute directly to the determination of tidal properties of the Jovian system during ephemeris generation. However, as discussed in Section 2.4, the Doppler tracking data from 3GM and PRIDE will allow $|k_2|^{(4,0)}$ to be determined.

The tidal dissipation inside the Galilean satellites at the forcing frequencies of the other satellites has only a small prefit r.m.s. residual for the orbit of Ganymede. The strongest inter-moon tidal influence on the dynamics of Ganymede is due to the Io- and Europa-raised tides on Ganymede, which both have an r.m.s. prefit residual that is even smaller than the Jupiter-raised tide on Ganymede. Considering the small postfit residual in Ganymede's orbit of this tide (Table 5), the inter-moon tides will not be visible for JUICE tracking data. Therefore, constraining the moons' dissipation at multiple forcing frequencies will not be possible with JUICE-derived ephemerides.

In addition to the residuals of the simulations for the dissipation, Table 5 also shows the pre- and postfit residuals of the influence of the static tide Love number k_2 of both Jupiter and the Galilean moons. Despite the high prefit influence of the non-dissipative tide (0.1, 1, 10 and 20 km for Callisto, Ganymede, Europa and Io, respectively), the postfit contribution is negligible in most cases relevant for JUICE (<0.5 m for Callisto, $\lesssim$5 m for Ganymede, <20 m for Europa, <100 m for Io). However, we do note that the time-behaviour of the postfit residual of Ganymede of the simulation for $k_2^{(1,0)}$ shows essentially no trend (Fig. 4) and it is possible that the 6-month m-level accurate observations of JUICE during the Ganymede orbit phase can be used to infer meaningful information on Io's static Love number (at the once-*per*-orbit forcing frequency). However, we also note that the results shown here are valid for a nominal $k_2 = 0.3$, with extreme values of its magnitude (based on geophysical modelling) of 0.04 and 0.8 (Lainey et al., 2009). Therefore, a measurement of Io's k_2 may be able to exclude certain interior models, if the real error of its estimate σ_{k_2} is below 0.8. We note that such a measurement will be uniquely achievable using active tracking techniques, as (Earth-based) astrometric observations will not be able to distinguish this periodic signal at the ~10 m level. Fig. 4 also shows the postfit behaviour of the influence of $k_2^{(3,0)}$, which may be very weakly observable if the orbit of JUICE is reconstructed exceptionally well during the flybys. However, Ganymede's tidal properties will be much more accurately determined from JUICE tracking data directly (Section 2.4).

4.4. Rotation models

Table 6 shows the r.m.s. pre- and postfit sensitivities of the orbits of the Galilean moons for the inclusion of the non-zero once-*per*-orbit ψ_j variations (see Table 1). It can be seen that the postfit residuals are unlikely to be at an observable level for any of the moons (postfit signatures of 25 m, 5 m, and 2 m for Europa, Ganymede and Callisto,

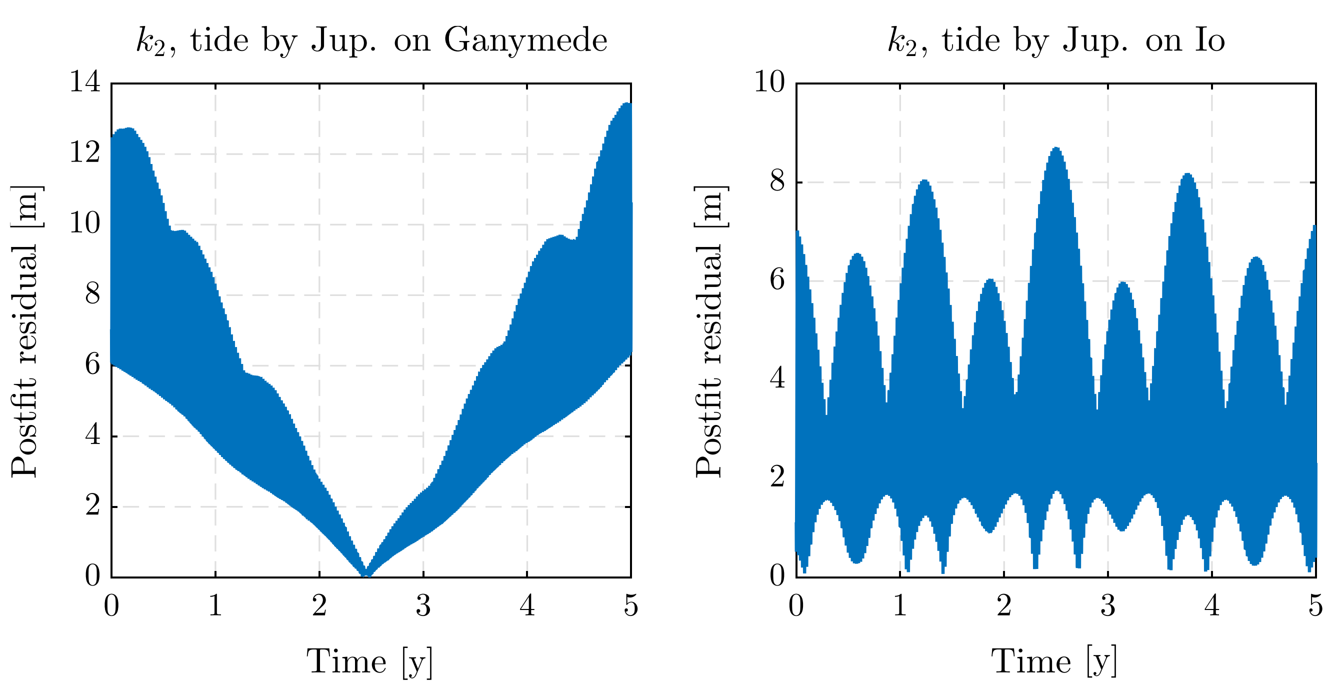

Fig. 4. Sensitivity of Ganymede's position to the k_2 Love numbers of the tides raised by Jupiter on Io and Ganymede.

Table 6
Pre- and post fit r.m.s. position residuals for Galilean moon rotation parameters (only residuals >0.1 m shown).

	r.m.s. prefit residuals [m]				r.m.s. postfit residuals [m]			
	Io	**Europa**	**Ganymede**	**Callisto**	**Io**	**Europa**	**Ganymede**	**Callisto**
ψ_1	4175.85	3776.54	1784.38	0.39	156.43	23.52	5.45	–
ψ_2	327.84	161.68	122.55	–	0.99	20.59	1.51	–
ψ_3	0.23	3.33	12.14	0.16	0.44	1.14	5.52	–
ψ_4	–	–	–	3.45	–	–	–	1.72

respectively). However, the influence of the rotation of Ganymede and Io may become relevant for accurate data analysis during the Ganymede orbit phase, where the orbit determination accuracy should be at the m-level. Both parameters show behaviour that has a substantial periodic component, as was the case for $(k_2)^{(1,0)}$ (Section 4.3). In fact, the time-behaviour of the postfit residuals for $\psi_{1;3}$ is very similar to that of $k_2^{(1;3,0)}$ (shown in Fig. 4).

However, the physical information that could be retrieved from the moons' rotations is in the libration amplitude γ_j, not the angle ψ_j, where $\gamma_j \ll \psi_j$ (see Section 2.2). Therefore, we can conclude that no estimates of rotational parameters of the moons can be made from the ephemerides that would improve our knowledge of their interior structure. Moreover, the amplitude of ψ_3 will be measured to high accuracy by JUICE during the orbit phase (Section 2.4).

Nevertheless, the inclusion of the non-zero ψ_j of Ganymede and Io may be warranted to prevent their signature from spilling over into other parameters (k_2 Love numbers), when exploiting data from the Ganymede orbit phase. To robustly model the signature of the rotational dynamics of the Galilean moons in the JUICE tracking data reduction, it will be advisable to review the applicability of the first-order model that we apply here, and perform a coupled orbital-rotational propagation of the dynamics. Our analysis shows that, barring large increases in the influences of librations that such an approach may uncover, modelling only first-order effects will be sufficient, as even they are at the limit of observability.

5. Conclusions

We have described a model for the dynamics of the Galilean moons that captures the physical effects that are potentially relevant for the ephemerides created from tracking data of the JUICE mission. The PRIDE, 3GM and JANUS data will be strongly complementary to the existing Earth-based astrometric data, by combining long-periodic relatively coarse measurements (50–500 km over >100 years) with short-periodic highly accurate measurements obtained largely by 3GM (10 s of meters orbit reconstruction for the flybys; ~1 m for the Ganymede low orbit phase). This will be supplemented by PRIDE observations of the angular position of the spacecraft, allowing the out-of-plane position to be directly measured. The JANUS data will be crucial to constrain the orbits of Europa (for which only two closely spaced flybys are planned) and Io (for which no flybys will occur).

By simulating ideal three-dimensional measurements with a given perturbation/parameter-uncertainty turned on, and then estimating the ephemerides of the Galilean moons with these effects turned off, we have analyzed whether a given physical effect should be included in the analysis of JUICE data. Our simulations indicate that the nominal dynamical model of the Galilean moons is highly resilient in absorbing the influence of various dynamical effects, even at the level of measurement accuracy that will be attained by JUICE. This is a direct result of the fact that the influence of many such effects can, to first order, be modelled by a slight modification of the orbital elements of (one of) the moons. The second-order dynamical effects can in most cases not be observed from JUICE tracking data analysis, since the Laplace resonance makes the dynamics most versatile in absorbing such perturbations.

Also, we have verified that the uncertainty in the ephemeris of Jupiter will not influence the dynamics of the Galilean moons to a significant degree. Whether the ephemeris generation of Jupiter and the moons can robustly be performed separately, however, depends on whether the signature of the Jupiter ephemeris error in the Earth-based range/lateral position will spill into the estimation of the moon ephemerides (and associated parameters).

As opposed to most other parameters, the tidal dissipation in the Galilean moons as well as in Jupiter, quantified by their k_2/Q, is only weakly absorbed into the nominal dynamics. The dissipation inside Io will be observable in the dynamics of Ganymede, allowing for an improved estimation of the dissipation, especially when combined with the existing astrometric data. Furthermore, a weak constraint could possibly be placed on the dissipation inside Europa. The observability of this effect will likely depend strongly on the combined observations of the dynamics of Ganymede and Europa/Io. Unfortunately, the dynamics of the Galilean moons is not sufficiently sensitive to inter-moon tides to allow for a determination of tidal properties of the moons at multiple forcing frequencies. Furthermore, the determination of k_2 separately from k_2/Q may be achievable for Io, although very weakly. Combining JUICE results on the Galilean moons with Juno-derived results on the tidal characteristics of Jupiter could allow for a robust decorrelation of the dissipation inside Jupiter and Io.

The signature of the rotational dynamics of the moons will be insufficiently strong to infer constraints on the moons' physical characteristics. However, it is advisable to perform a coupled orbital-rotational model of the Galilean satellites, to be able to robustly include the signature of rotation in the ephemerides, without this signature spilling over into the estimation of other parameters.

In this work, we have provided clear guidelines for the viability of the estimation of a wide range of parameters, thereby elucidating the science case of the instruments that provide these data and providing a clear focus for further development and observation planning of these instruments. The limited number of parameters that cannot be absorbed into the initial states means that the generation of ephemerides from JUICE range and (optical and radio) astrometry data will only need to incorporate the estimation of a limited set of additional parameters.

Finally, our results highlight the strong synergy between the various missions to the Jovian system (JUICE, Juno, EMFM). The focus of Juno on the properties of Jupiter allows for a crucial decorrelation of Jupiter's and the moons' properties during the parameter estimation. The combined data analysis of JUICE and EMFM will facilitate the decorrelation of various dynamical signatures in the Jovian system, by exploiting accurate direct measurements of both Ganymede and Europa. This synergy also extends to other missions to the Jovian system that are under investigation, strengthening their science case since the data they will collect could very well improve the science return from existing data.

Our simulations do not include an assessment of the JUICE tracking data inversion, but provide an overview of potentially observable parameters. We will investigate the quantitative ephemeris generation from JUICE tracking data and Earth-based astrometry in future work.

Acknowledgements

DD thanks Hermes Jara Orue for fruitful discussions on the dynamics, tides and rotations of the Galilean moons. The authors thank Luciano Iess of the 3GM team for fruitful discussions on the JUICE mission and its science objective. This work was supported by the Centre National d'Etudes Spatiales (CNES). Two anonymous reviewers are thanked for a careful reading of the manuscript, which has greatly improved manuscript.

References

Acton, C., 1996. Ancillary data services of nasa's navigation and ancillary information facility. Planet. Space Sci. 44 (1), 65–70.
Anderson, J.D., Schubert, G., Jacobson, R.A., Lau, E.L., Moore, W.B., Palguta, J.L., 2004. Discovery of mass anomalies on Ganymede. Science 305, 989–991.
Anderson, J.D., Johnson, T.V., Schubert, G., Asmar, S., Jacobson, R.A., Johnston, D., Lau, E.L., Lewis, G., Moore, W.B., Taylor, A., Thomas, P.C., Weinwurm, G., 2005. Amalthea's density is less than that of water. Science 308, 1291–1293.
Antreasian, G., Ardalan, S., Bordi, J., Criddle, K., Ionasescu, R., Jacobson, R., Jones, J., MacKenzie, R., Parcher, D., Pelletier, F., Roth, D., Thompson, P., Vaughan, A., 2008. Cassini orbit determination results: January 2006-end of prime mission. In: AIAA/AAS Astrodynamics Specialist Conference (AIAA 2008-6747), Honolulu, Hawai.
Archinal, B.A., A'Hearn, M.F., Bowell, E., Conrad, A., Consolmagno, G.J., Courtin, R., Fukushima, T., Hestroffer, D., Hilton, J.L., Krasinsky, G.A., Neumann, G., Oberst, J., Seidelmann, P.K., Stooke, P., Tholen, D.J., Thomas, P.C., Williams, I.P., 2011. Report of the IAU working group on cartographic coordinates and rotational elements: 2009. Celest. Mech. Dyn. Astron. 109, 101–135.
Arlot, J.-E., Desmars, J., Lainey, V., Robert, V., 2012. The astrometry of the natural planetary satellites applied to their dynamics before and after Gaia. Planet. Space Sci. 73, 66–69.
Auclair-Desrotour, P., Le Poncin-Lafitte, C., Mathis, S., 2014. Impact of the frequency dependence of tidal Q on the evolution of planetary systems. Astron. Astrophys. 561, L7.
Beauvalet, L., Lainey, V., Arlot, J.-E., Binzel, R.P., 2012. Dynamical parameter determinations in pluto's system. Expected constraints from the New Horizons mission to Pluto. Astron. Astrophys. 540, A65.
Bills, B.G., 2005. Free and forced obliquities of the Galilean satellites of Jupiter. Icarus 175, 233–247.
Boué, G., Correia, A.C., Laskar, J., 2016. Complete spin and orbital evolution of close-in bodies using a Maxwell viscoelastic rheology. Celest. Mech. Dyn. Astron. 126 (1), 31–60.
Campbell, J.K., Synnott, S.P., 1985. Gravity field of the Jovian system from Pioneer and Voyager tracking data. Astron. J. 90, 364–372.
Christou, A.A., Lewis, F., Roche, P., Hidas, M.G., Brown, T.M., 2010. Observational detection of eclipses of J5 amalthea by the galilean satellites. Astron. Astrophys. 522, A6.
Comstock, R.L., Bills, B.G., 2003. A solar system survey of forced librations in longitude. J. Geophys. Res. (Planets) 108, 5100.
Curkendall, D.W., Border, J.S., 2013. Delta-DOR: the one-nanoradian navigation measurement system of the deep space network – history, architecture, and componentry. Interplanet. Netw. Prog. Rep. 42 (193), D1.
Deienno, R., Nesvorný, D., Vokrouhlický, D., Yokoyama, T., 2014. Orbital perturbations of the Galilean satellites during planetary encounters. Astron. J. 148, 25.
Dirkx, D., Vermeersen, L., Noomen, R., Visser, P., 2014. Phobos laser ranging: numerical geodesy experiments for Martian system science. Planet. Space Sci. 99, 84–102.
Dirkx, D., 2015. Interplanetary Laser Ranging – Analysis for Implementation in Planetary Science Mission (Ph.D. Thesis), Delft University of Technology.
Duev, D.A., Molera Calvés, G., Pogrebenko, S.V., Gurvits, L.I., Cimó, G., Bocanegra Bahamon, T., 2012. Spacecraft VLBI and doppler tracking: algorithms and implementation. Astron. Astrophys. 541, A43.
Efroimsky, M., Lainey, V., 2007. Physics of bodily tides in terrestrial planets and the appropriate scales of dynamical evolution. J. Geophys. Res. (Planets) 112, 12003.
Emelyanov, N.V., 2005. The mass of Himalia from the perturbations on other satellites. Astron. Astrophys. 438, L33–L36.
Emelyanov, N.V., Arlot, J.-E., 2008. The natural satellites ephemerides facility MULTI-SAT. Astron. Astrophys. 487, 759–765.
Fienga, A., Laskar, J., Morley, T., Manche, H., Kuchynka, P., Le Poncin-Lafitte, C., Budnik, F., Gastineau, M., Somenzi, L., 2009. INPOP08, a 4-D planetary ephemeris: from asteroid and time-scale computations to ESA mars express and venus express contributions. Astron. Astrophys. 507, 1675–1686.
Fienga, A., Manche, H., Laskar, J., Gastineau, M., Verma, A., 2014. INPOP New Release: INPOP13b. ArXiv e-prints.
Finnocchiaro, S., 2012. Numerical Simulations of the Juno Gravity Experiment (Ph.D. Thesis). Sapienza Università di Roma.
Folkner, W.M., 2011. Uncertainties in the JPL planetary ephemeris. In: Capitaine, N. (Ed.), Journées Systèmes de Référence Spatio-temporels 2010, 43–48.
Folkner, W.M., Williams, J.G., Boggs, D.H., Park, R.S., Kuchynka, P., 2014. The planetary and lunar ephemerides DE430 and DE431. Interplanet. Netw. Prog. Rep. 42 (196), C1.
Fomalont, E.B., Goss, W.M., Beasley, A.J., Chatterjee, S., 1999. Sub-milliarcsecond precision of pulsar motions: using in-beam calibrators with the VLBA. Astron. J. 117, 3025–3030.
Grasset, O., Dougherty, M.K., Coustenis, A., Bunce, E.J., Erd, C., Titov, D., Blanc, M., Coates, A., Drossart, P., Fletcher, L.N., Hussmann, H., Jaumann, R., Krupp, N., Lebreton, J.-P., Prieto-Ballesteros, O., Tortora, P., Tosi, F., Van Hoolst, T., 2013. JUpiter ICy moons explorer (JUICE): an ESA mission to orbit Ganymede and to characterise the jupiter system. Planet. Space Sci. 78, 1–21.
Greenberg, R., 1987. Galilean satellites – evolutionary paths in deep resonance. Icarus 70, 334–347.
Greenberg, R., 2010. The icy Jovian satellites after the Galileo mission. Rep. Prog. Phys. 73 (3), 036801.
Gurvits, L.I., Bocanegra Bahamon, T.M., Cimò, G., Duev, D.A., Molera Calvés, G., Pogrebenko, S. V., de Pater, I., Vermeersen, L.L.A., Rosenblatt, P., Oberst, J., Charlot, P., Frey, S., Tudose, V., 2013. Planetary radio interferometry and doppler experiment (PRIDE) for the JUICE mission. European Planetary Science Congress 2013, vol. 8, p. 357.
Hees, A., Folkner, W.M., Jacobson, R.A., Park, R.S., 2014. Constraints on modified newtonian dynamics theories from radio tracking data of the cassini spacecraft. Phys. Rev. D 89 (10), 102002.
Heller, R., Marleau, G.-D., Pudritz, R.E., 2015. The formation of the Galilean moons and Titan in the Grand Tack scenario. Astron. Astrophys. 579, L4.
Horiuchi, S., Clark, J., García-Miró, C., Goohart, C., Jacobs, C., Madde, R., Mercolino, M., Naudet, C., Snedeker, L., Sotuela, I., et al., 2013. The X/Ka celestial reference frame: results from combined nasa-ESA baselines. In: Asia-Pacific Radio Astronomy Conference.
Iess, L., Benedetto, M.D., James, N., Mercolino, M., Simone, L., Tortora, P., 2014. Astra: interdisciplinary study on enhancement of the end-to-end accuracy for spacecraft tracking techniques. Acta Astronaut. 94 (2), 699–707.
Iess, L., Jacobson, R.A., Ducci, M., Stevenson, D.J., Lunine, J.I., Armstrong, J.W., Asmar, S.W., Racioppa, P., Rappaport, N.J., Tortora, P., 2012. The tides of Titan. Science 337 (6093), 457–459.
Iess, L., 2013. 3GM: gravity and geophysics of Jupiter and the Galilean Moons. European Planetary Science Congress 2013, 8, pp. 491.
IMCCE, 2010. NOE-5-2010-GAL-a.bsp SPICE Kernel. ⟨ftp://ftp.imcce.fr/pub/ephem/satel/galilean/L2/⟩, (last accessed 20.08.15).
Iorio, L., Lainey, V., 2005. The Lense-Thirring effect in the Jovian system of the Galilean satellites and its measurability. Int. J. Mod. Phys. D 14, 2039–2049.
Jacobson, R.A., 2004. The orbits of the major Saturnian satellites and the gravity field of saturn from spacecraft and Earth-based observations. Astron. J. 128, 492–501.
Jacobson, R.A., 2014. The orbits of the Uranian satellites and rings, the gravity field of the Uranian system, and the orientation of the pole of Uranus. Astron. J. 148, 76.
Jacobson, R.A., 2001. The Gravity Field of the Jovian System and the Orbits of the Regular Jovian Satellites. In: Proceedings of the AAS/Division for Planetary Sciences Meeting Abstracts, vol. 33, p. 1039.
Jacobson, R.A., 2013. The gravitational fields of the Galilean Satellites – revisited. Volume 45 of AAS/Division for Planetary Sciences Meeting Abstracts, vol. 6, p. 418.
Jacobson, R.A., Folkner, W.M., 2014. The Tidal Perturbations of the Galilean Satellites. Volume 46 of AAS/Division for Planetary Sciences Meeting Abstracts, vol. 3, p. 418.
Jaumann, R., Palumbo, P., Hoffmann, H., Cremonese, G., Lara, L., Della Corte, V., Schmitz, N., Debei, S., Michaelis, H., Lichopoj, A., Magrin, D., Mazzotta Epifanti, E., Mottola, S., Ragazzoni, R., Zusi, M., Holland, A., 2013. JANUS on the JUICE mission: the camera to investigate Ganymede, Europa, Callisto and the Jovian system. In: Proceedings of the European Planetary Science Congress 2013, vol. 8, p. 506.
Jones, D.L., Folkner, W.M., Jacobson, R.A., Jacobs, C.S., Dhawan, V., Romney, J., Fomalont, E., 2015. Astrometry of cassini with the VLBA to improve the saturn ephemeris. Astron. J. 149, 28.
Kaula, W.M., 1964. Tidal dissipation by solid friction and the resulting orbital evolution. Rev. Geophys. Space Phys. 2, 661–685.
Lainey, V., 2016. Quantification of tidal parameters from solar system data. Celest. Mech. Dyn. Astron. 126 (1), 145–156.
Lainey, V., Tobie, G., 2005. New constraints on Io's and Jupiter's tidal dissipation. Icarus 179, 485–489.
Lainey, V., Vienne, A., Duriez, L., 2001. New estimation of usually neglected forces acting on Galilean system. Celest. Mech. Dyn. Astron. 81, 115–122.
Lainey, V., Arlot, J.E., Vienne, A., 2004a. New accurate ephemerides for the Galilean satellites of jupiter. II. Fitting the observations. Astron. Astrophys. 427, 371–376.
Lainey, V., Duriez, L., Vienne, A., 2004b. New accurate ephemerides for the Galilean satellites of jupiter. I. Numerical integration of elaborated equations of motion. Astron. Astrophys. 420, 1171–1183.
Lainey, V., Dehant, V., Pätzold, M., 2007. First numerical ephemerides of the Martian moons. Astron. Astrophys. 465, 1075–1084.
Lainey, V., Arlot, J.-E., Karatekin, Ö, van Hoolst, T., 2009. Strong tidal dissipation in Io and Jupiter from astrometric observations. Nature 459, 957–959.
Lainey, V., Karatekin, Ö, Desmars, J., Charnoz, S., Arlot, J.-E., Emelyanov, N., Le Poncin-Lafitte, C., Mathis, S., Remus, F., Tobie, G., Zahn, J.-P., 2012. Strong tidal dissipation in saturn and constraints on Enceladus' thermal state from astrometry. Astrophys. J. 752, 14.
Lainey, V., Jacobson, R.A., Tajeddine, R., Cooper, N.J., Murray, C., Robert, V., Tobie, G., Guillot, T., Mathis, S., Remus, F., et al., 2015. New Constraints on Saturn's Interior from Cassini Astrometric Data. arXiv preprint arXiv:1510.05870.
Lainey, V., van Hoolst, T., 2009. Jovian tidal dissipation from inner satellite dynamics. In: Proceedings of the European Planetary Science Congress 2009, p. 392.
Lanyi, G., Bagri, D.S., Border, J., 2007. Angular position determination of spacecraft by

radio interferometry. IEEE Proc. 95 (11), 2193–2201.
Le Maistre, S., Folkner, W., Jacobson, R., Serra, D., 2016. Jupiter spin-pole precession rate and moment of inertia from Juno radio-science observations. Planet. Space Sci., 78–92.
Lieske, J.H., 1980. Improved ephemerides of the Galilean satellites. Astron. Astrophys. 82, 340–348.
Lieske, J.H., 1998. Galilean satellite ephemerides E5. Astron. Astrophys. Suppl. 129, 205–217.
Majid, W.A., Bagri, D.S., 2008. Precision spacecraft tracking using in-beam phase referencing. In: Proceedings of the IEEE Aerospace Conference, pp. 1–8.
Malhotra, R., 1991. Tidal origin of the laplace resonance and the resurfacing of ganymede. Icarus 94, 399–412.
Malkin, Z., Jacobs, C., Arias, F., Boboltz, D., B¨ohm, J., Bolotin, S., Bourda, G., Charlot, P., de Witt, A., Fey, A., Gaume, R., Gordon, D., Heinkelmann,R., Lambert, S., Ma, C., Nothnagel, A., Seitz, M., Skurikhina,E., Souchay, J., Titov, O., 2015. The ICRF-3: Status, plans, andprogress on the next generation International Celestial Reference Frame. In: Malkin, Z., Capitaine, N., (Eds.), Journ´ees 2014 "Syst`emes der´ef´erence spatio-temporels", pp. 3–8.
Mathis, S., Le Poncin-Lafitte, C., 2009. Tidal dynamics of extended bodies in planetary systems and multiple stars. Astron. Astrophys. 497, 889–910.
Mazarico, E., Genova, A., Neumann, G.A., Smith, D.E., Zuber, M.T., 2015. Simulated recovery of Europa's global shape and tidal love numbers from altimetry and radio tracking during a dedicated flyby tour. Geophys. Res. Lett. 42 (9), 3166–3173.
McEwen, A., Turtle, E., Hibbard, K., Reynolds, E., Adams, E., 2014. Io Volcano observer (IVO): budget travel to the outer solar system. Acta Astronaut. 93, 539–544.
Mignard, F., 1980. The evolution of the lunar orbit revisited. II. Moon Planets 23, 185–201.
Milani, A., Gronchi, G., 2010. Theory of orbit determination. In: Theory of Orbit Determination, Cambridge University Press.
Montenbruck, O., Gill, E., 2000. Satellite Orbits: Models, Methods, and Applications. Physics and Astronomy Online Library. Springer Verlag, Berlin Heidelberg.
Morgado, B., Assafin, M., Vieira-Martins, R., Camargo, J., Dias-Oliveira, A., Gomes-Júnior, A., 2016. Astrometry of mutual approximations between natural satellites. application to the Galilean moons. Mon. Not. R. Astron. Soc. 460 (4), 4086–4097.
Parisi, M., Finocchiaro, S., Iess, L., 2012. Multi-arc and batch-sequential filters for the orbit determination of ESA's JUICE mission. In: Proceedings of the 23rd International Symposium on Space Flight Dynamics.
Parisi, M., Iess, L., Finocchiaro, S., 2014. The gravity fields of Ganymede, Callisto and Europa: how well can JUICE do? In: EGU General Assembly Conference Abstracts, vol. 16, p. 11758.
Park, R.S., Bills, B., Buffington, B.B., Folkner, W.M., Konopliv, A.S., Martin-Mur, T.J., Mastrodemos, N., McElrath, T.P., Riedel, J.E., Watkins, M.M., 2015. Improved detection of tides at Europa with radiometric and optical tracking during flybys. Planet. Space Sci..
Pasewaldt, A., Oberst, J., Willner, K., Wählisch, M., Hoffmann, H., Matz, K.-D., Roatsch, T., Hussmann, H., Lupovka, V., 2012. New astrometric observations of Deimos with the SRC on Mars Express. Astron. Astrophys. 545, A144.
Peale, S.J., 1999. Origin and evolution of the natural satellites. Annu. Rev. Astron. Astrophys. 37, 533–602.
Peale, S.J., Lee, M.H., 2002. A primordial origin of the Laplace relation among the Galilean satellites. Science 298, 593–597.
Pitjeva, E.V., 2001. Modern numerical ephemerides of planets and the importance of ranging observations for their creation. Celest. Mech. Dyn. Astron. 80, 249–271.
Rambaux, N., van Hoolst, T., Karatekin, Ö, 2011. Librational response of Europa, Ganymede, and Callisto with an ocean for a non-keplerian orbit. Astron. Astrophys. 527, A118.
Robert, V., Lainey, V., Pascu, D., Pasewaldt, A., Arlot, J.-E., De Cuyper, J.-P., Dehant, V., Thuillot, W., 2015. A new astrometric measurement and reduction of USNO photographic observations of Phobos and Deimos: 1967–1997. Astron. Astrophys. 582, A36.
Robert, V., de Cuyper, J.-P., Arlot, J.-E., de Decker, G., Guibert, J., Lainey, V., Pascu, D., Winter, L., Zacharias, N., 2011. A new astrometric reduction of photographic plates using the DAMIAN digitizer: improving the dynamics of the jovian system. Mon. Not. R. Astron. Soc. 415, 701–708.
Schubert, G., Anderson, J.D., Spohn, T., McKinnon, W.B., 2004. Interior composition, structure and dynamics of the Galilean satellites. In: Bagenal, F., Dowling, T.E., McKinnon, W.B. (Eds.), Jupiter. The Planet, Satellites and Magnetosphere, pp. 281–306.
Titov, D., Barabash, S., Bruzzone, L., Dougherty, M., Erd, C., Fletcher, L., Gare, P., Gladstone, R., Grasset, O., Gurvits, L., Hartogh, P., Hussmann, H., Iess, L., Jaumann, R., Langevin, Y., Palumbo, P., Piccioni, G., Wahlund, J.-E., 2014. JUICE: complementarity of the payload in adressing the mission science objectives. In: EGU General Assembly Conference Abstracts, Volume 16 of EGU General Assembly Conference Abstracts, p. 13471.
Titov, D., Grasset, O., Fletcher, L., SWT, J., 2014. JUICE Science Requirements Document. JUI-EST-SGS-RS-001.
Tragesser, S.G., Longuski, J.M., 1999. Modeling issues concerning motion of the Saturnian satellites. J. Astronaut. Sci. 47 (3–4), 275–294.
Van Hoolst, T., Baland, R.-M., Trinh, A., 2013. On the librations and tides of large icy satellites. Icarus 226, 299–315.
Yoder, C.F., Peale, S.J., 1981. The tides of Io. Icarus 47, 1–35.